ISSN 0454－4641

運輸省港湾技術研究所

港湾技術研究所報告

REPORT OF THE PORT AND HARBOUR RESEARCH INSTITUTE

MINISTRY OF TRANSPORT

VOL.39 NO.4 Dec. 2000

NAGASE, YOKOSUKA, JAPAN

港湾技術研究所報告（REPORT OF P. H. R. I.）
第 39 巻　第 4 号（Vol. 39, No. 4），　2000年12月（Dec. 2000）

目　　次（CONTENTS）

REPORT OF THE PORT AND
HARBOUR RESEARCH INSTITUTE
Vol.39,No.4(Dec.2000)

Medium-Term Bar Movement and Sediment Transport at HORS

Yoshiaki KURIYAMA*

Synopsis

Medium-term bar movement and the associated sediment transport were investigated with beach profiles measured in the field; the data were obtained nearly daily for eight years from the foot of a dune to a water depth of about 5 m at Hazaki Oceanographical Research Station (HORS). As a result, the bar crest was found to migrate seaward repeatedly with a period of a year. The cross-shore sediment transport, on the other hand, seasonally fluctuated seaward and shoreward during the seaward migration of the bar crest. The empirical eigenfunction analysis applied to the beach profile data showed that the bar crest migration was almost independent of the topography change in the foreshore. The influence of the wave energy flux in deep water on the cross-shore sediment movement was also investigated.

Key Words: longshore bar, cross-shore sediment transport, empirical eigenfunction analysis, HORS

* Chief of Littoral Drift Laboratory, Marine Environment Division
Nagase 3-1-1, Yokosuka, Kanagawa 239-0826, Japan
Phone: +81-468-44-5012, Fax: +81-468-41-9812, E-mail: kuriyama@cc.phri.go.jp

港湾技術研究所報告
第39巻第4号(2000.12)

波崎海洋研究施設で観測された沿岸砂州の長期変動特性と底質移動特性

栗山　善昭*

要　旨

鹿島灘に面する波崎海洋研究施設（HORS）において後浜から外浜にかけてほぼ毎日観測された8年間の断面データを基に，沿岸砂州（バー）の長期変動特性，ならびにその特性と前浜の地形変化や底質移動との関係を検討した．その結果，バーの頂部は約1年のサイクルで沖向きに移動すること，このバーの移動と前浜の地形変化とは独立であること，バー頂部は沖向きに移動するものの各地点の岸沖漂砂は同じく約1年の周期で沖向き，岸向きに変動することが明らかとなった．さらに，このバーの移動に伴う岸沖漂砂の変動特性と外力である沖波のエネルギーフラックスとの関係を検討し，両者の関係を明らかにした．

キーワード：沿岸砂州，岸沖漂砂，経験的固有関数法，HORS

* 海洋環境部　漂砂研究室長
〒239-0826　横須賀市長瀬3－1－1　運輸省港湾技術研究所
電話：0468-44-5012,　Fax：0468-41-9812,　E-mail：kuriyama@cc.phri.go.jp

CONTENTS

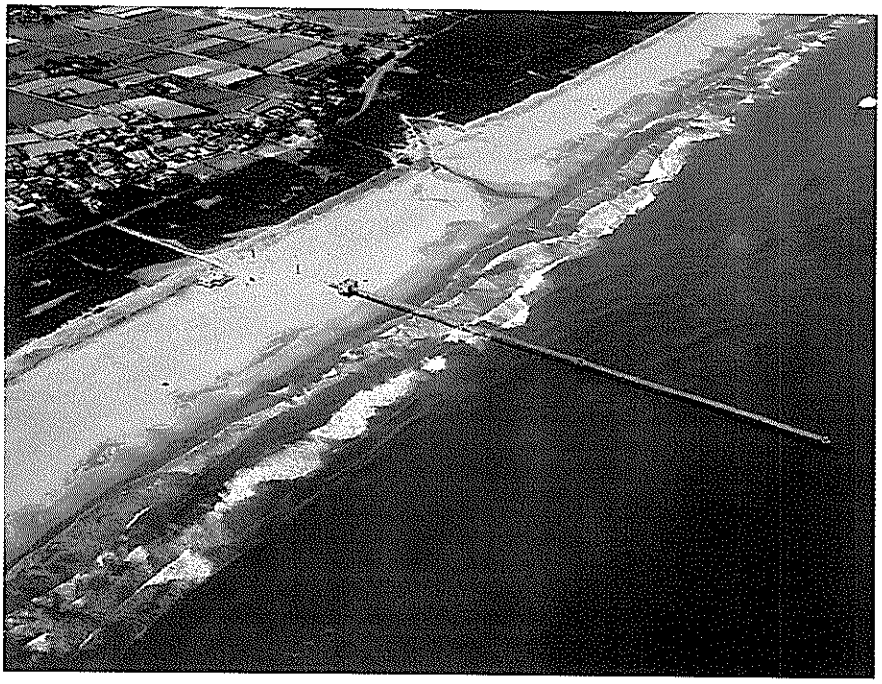

Photograph 1 Aerial view of HORS.

Photograph 2 Surveying in the backshore.

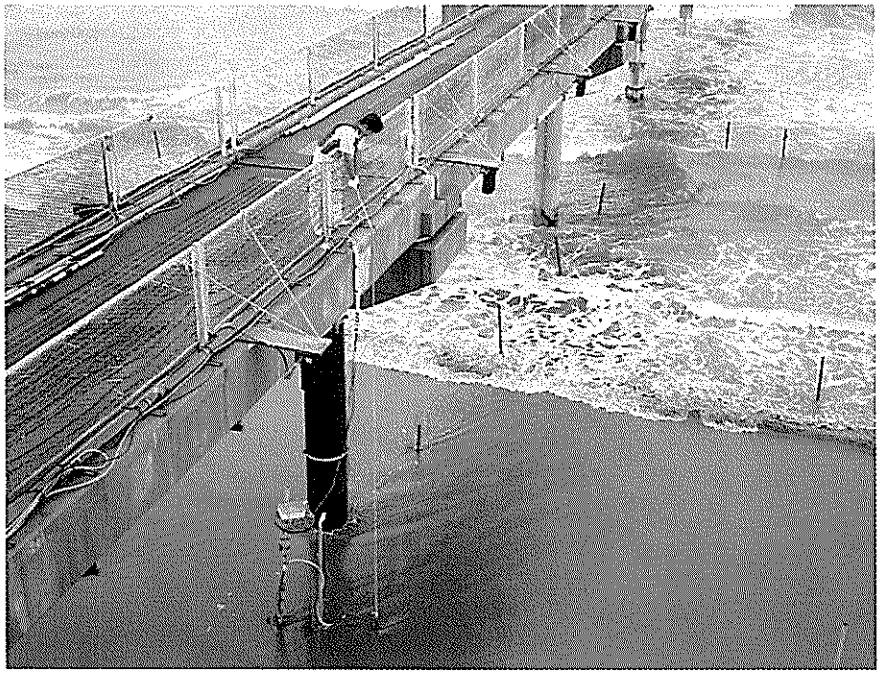

Photograph 3 Surveying from the pier.

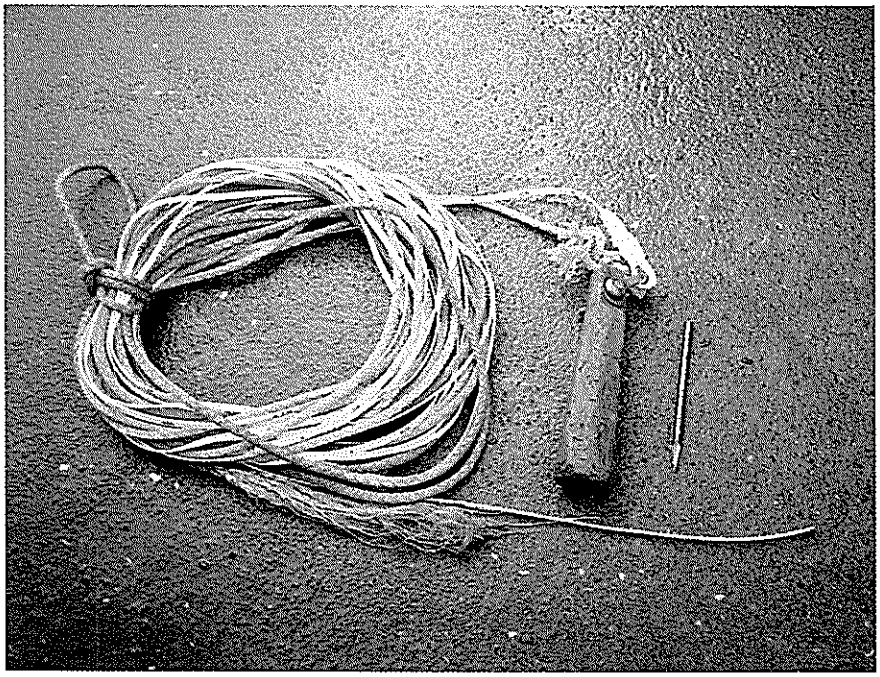

Photograph 4 5kg lead for surveying from the pier.

1. Introduction

The Coastal Act in Japan revised in 1999 encourages coastal management in a wide region, which is expected to extend between the two obvious boundaries that completely stop the sediment movement alongshore, and from a dune to a water depth of about 20 m cross-shore. Consequently, in the coastal management, not only topography change in the foreshore but also that in the nearshore is required to be considered. In the nearshore, topography change is larger than that in the foreshore owing to active sediment movement (*e.g.* Birkemeier, 1984; Katoh and Yanagishima, 1988), and longshore bars are frequently formed.

The importance of longshore bars in the coastal management was shown by Yamamoto and Sato (1998). They conducted experiments in a large flume to show that the shoreline on a barred beach, which normally advanced in mild wave conditions, did not advance even in a mild wave condition after the longshore bar was removed. This result indicates that the understanding of bar movement is important in the coastal management.

The understanding of bar movement is also required from another point of view. In the United States, Australia and Europe, an offshore nourishment technique has recently been developed as a cost effective nourishment method. In this nourishment, sediment is placed in the nearshore, and is expected to move shoreward or at least to stay there. Since the nourished sediment forms a bar, the understanding of bar movement is essential to establish the effective offshore nourishment technique. In Japan, although the offshore nourishment has not been performed yet, there is a possibility that it will be adopted in the near future as environment-friendly countermeasures against beach erosion.

Although the importance of the understanding of bar movement in the coastal management has been recognized recently, a lot of studies on bar movement have already been done since the 19th century (Komar, 1998). Recently, with long-term and medium-term topography data obtained with echo-sounding and video technique, long-term and medium-term bar movements on several coasts in the United States, the Netherlands and New Zealand have been investigated (Birkemeier, 1984; Lippmann et al., 1993; Ruessink and Kroon, 1994; Wijnberg and Terwindt, 1995; Shand and Bailey, 1999). These studies, however, focused on the bar behavior including generation, migration and decay of a bar, and little attention was paid to the sediment movement associated with the bar movement, which is important to the coastal management.

The relationship between the bar movement and the topography change in the foreshore was also rarely investigated except for Takeda and Sunamura (1992) and Stive et al. (1996). Furthermore, the effect of incident wave characteristics on the medium-term bar movement and the associated sediment transport is poorly understood although many studies on short-term bar movement and the wave characteristics have been carried out (*e.g.* Sallenger et al., 1985; Sallenger and Howd, 1989; Lippmann and Holman, 1990; Greenwood and Osborne, 1991; Sunamura and Takeda, 1993; Larson and Kraus, 1994; Kuriyama, 1996; Thornton et al., 1996; Plant and Holman, 1997; Gallagher et al., 1998; Aagaard and Greenwood, 1999; Miller et al., 1999). Recently, Plant et al. (1999) and Larson et al. (2000) investigated medium-term beach profile changes with the wave characteristics. Plant et al. (1999) proposed a model to predict the medium-term migration of a bar crest with the offshore wave height, and Larson et al. (2000) showed a high correlation between the beach profile and the ratio of wave breaking using canonical correlation analysis.

The objective of this study is to investigate medium-term bar movement, its influence on the topography change in the foreshore, the sediment movement associated with the bar movement and the relationship between the sediment movement and the incident wave characteristics on the basis of beach profile data obtained in the field.

2. Beach Profile Data

Beach profile data used in this study were obtained for eight years from January in 1987 to December in 1994 at Hazaki Oceanographical Research Station (HORS, **Photograph 1**), which has a field observation pier of 427 m in length on the Hasaki coast of Japan facing the Pacific Ocean; the location of HORS is shown in **Figure 1**. The beach

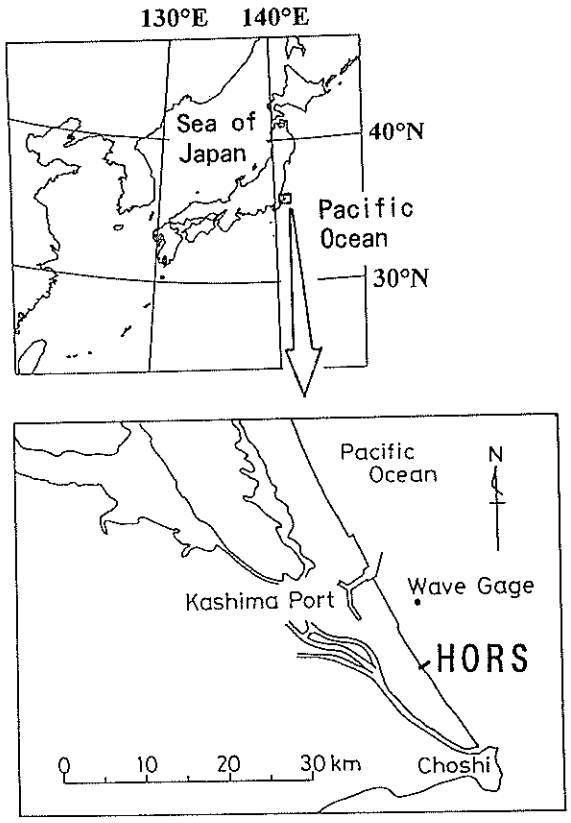

Figure 1 Location of HORS.

profiles along HORS were measured every 5 m every day except for weekends and holidays with a 5 kg lead from the pier and with a level and a staff shoreward of the pier (**Photographs 2** to **4**).

The upper part of **Figure 2** shows the mean beach profile and the maximum and minimum values of elevation from 1987 to 1994, and the lower one shows the standard deviation of elevation. The elevation is based on the datum level in Hasaki. The high, the mean and the low water levels based on the datum level are 1.252 m, 0.651 m, and –0.196 m, respectively. Since a local scour occurs around a piling supporting the pier deck of HORS, the elevations measured at the survey points close to the pilings were replaced by the values interpolated with the elevations measured where the effects of the scours were negligible shoreward and seaward of the pilings; the survey points close to pilings are located where the offshore distances are 100, 105, 165, 175, 200, 205, 220, 235, 250, 265, 280, 295, 310, 325, 340, 355, 370 and 385 m.

The mean beach slope in the area where the offshore distance is –60 m to 200 m is about 1/50, and the slope seaward of the area is about 1/200. The standard deviation of elevation increases seaward from around the point where the offshore distance is 20 m (referred to as P20m), has a peak around at P210m, and then gradually decreases to P380m.

3. Alongshore Uniformity of Topography around HORS and Influence of Pilings

Before the analysis of the beach profile data at HORS, the alongshore uniformity of the topography around HORS and the influence of the pilings on the topography were examined with seventeen topographic maps around HORS; these maps were obtained from November in 1986, when the influence of the construction work of HORS on the

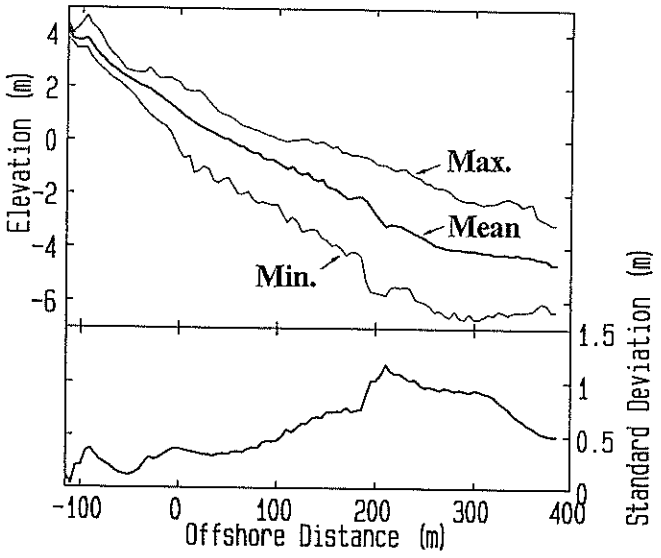

Figure 2 Mean beach profile, maximum and minimum elevations, and standard deviation of elevation at HORS.

topography is assumed to be small, to August in 1998. Besides the daily surveying at HORS, the bottom topography around HORS was surveyed once or twice a year in the area of 600 m alongshore and about 700 m cross-shore. **Figure 3** is a contour map of the mean topography estimated with the seventeen maps. The alongshore interval of the survey lines expanding cross-shore was 50 m, and the cross-shore intervals of the survey points were 10 m and 20 m shoreward and seaward of the points where the offshore distance was 150 m, respectively.

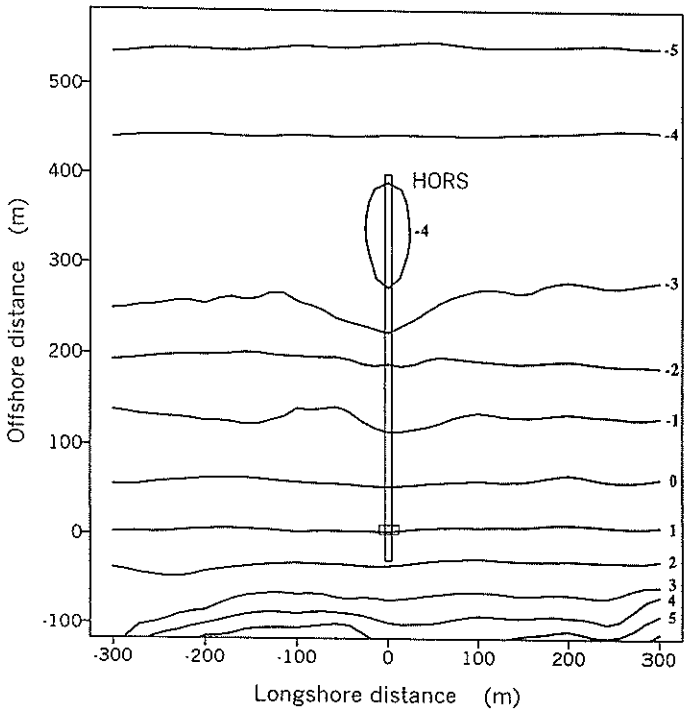

Figure 3 Mean topography around HORS.

Figure 4 shows the mean beach profiles and the standard deviations of elevation along HORS and along the six survey lines located 200 m to 300 m north and south of HORS. Away from HORS, the mean elevations are in close agreement, and so are the standard deviations. This result indicates that the topography around HORS was generally uniform alongshore.

Along HORS, however, from P200m to P400m, the mean elevation is lower and the standard deviation is larger than those away from HORS. This is considered to be caused by local scours around pilings. Nevertheless, the beach profile data along HORS can be used for the investigation on medium-term beach profile change at Hasaki if the beach profile change along HORS qualitatively agrees with that away from HORS. Thus, the relationship between the beach profiles along HORS and those away from HORS was further investigated.

Figure 5 shows the comparison between elevations from P20m to P360m at HORS and those in a north and a south regions of HORS; the north and the south regions cover the areas 200 m to 300 m north and south of HORS,

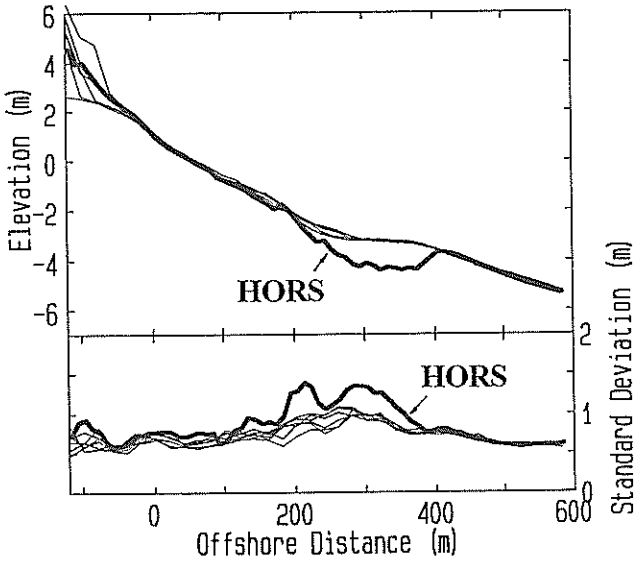

Figure 4 Mean beach profiles and standard deviations estimated along HORS and 200 m to 300 m north and south of HORS. (Thick lines show the values along HORS.)

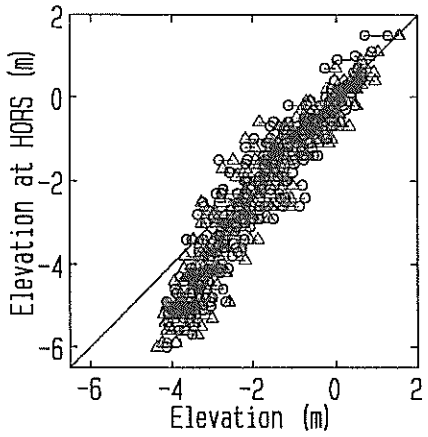

Figure 5 Comparison between elevations at HORS and those in the north and the south regions. (Open circles and triangles show the values in the north and the south regions, respectively.)

respectively. The values in the north region are the mean values of the elevations along the three survey lines in the region, and so are the values in the south region. In the area where the elevations at HORS are higher than –2 m, the elevations at HORS are approximately equal to those away from HORS. In the area where the elevations at HORS are lower than –2 m, on the other hand, the values at HORS are lower than the values away from HORS. However, those are highly correlated. This result suggests that the beach profile change at HORS qualitatively agreed with that away from HORS.

Then, as parameters representing beach profiles on barred beaches, the elevations and the locations of a bar crest and a trough were chosen, and the parameters along HORS and those in the north and the south regions were compared. The bar crest and the trough were defined to be the points that had the local maximum and minimum elevations, respectively, and formed a bar whose height, difference in elevation between a bar crest and the shoreward trough, was over criteria; the local maximum and minimum elevations were defined to have a beach slope of zero estimated as the mean slope in the area of 60 m cross-shore. Since the standard deviation of elevation along HORS was larger than those away from HORS as shown in **Figure 4**, the criteria were set to be 50 cm along HORS and 30 cm away from HORS. The elevations and the locations of the bar crests and the troughs in the north and the south regions were estimated on the basis of the mean beach profiles in the regions.

Figures 6 (1) and **(2)** show comparisons of the elevations, the locations and the occurrence frequencies of the bar crests and the troughs along HORS and away from HORS. Middle panels show the frequencies of three cases in which

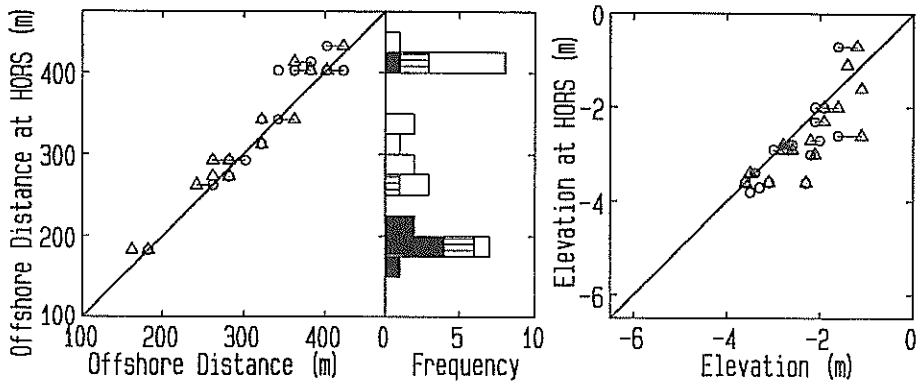

Figure 6 (1) Location, elevation and occurrence frequency of bar crest. (Open circles and triangles show the values in the north and the south regions. Middle panel shows the frequency of three cases in which bars were identified only along HORS (solid box), along HORS and in the north or the south region (hatched box), and in all three regions (open box).)

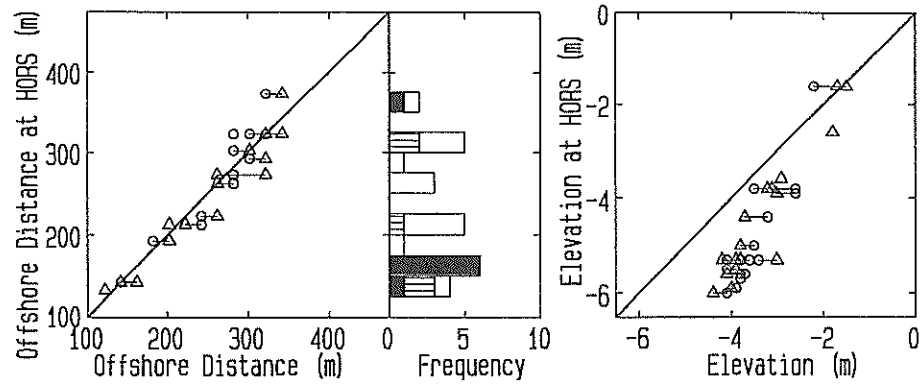

Figure 6 (2) Location, elevation and occurrence frequency of trough. (Details are as in **Figure 6 (1).**)

bars (or troughs) were identified only along HORS, along HORS and in the north or the south region, and in all three regions. When the topography is not uniform alongshore, a bar may be observed in a certain region but not in other region. Thus, the occurrence frequency also represents the alongshore uniformity of the topography.

As shown in **Figure 6 (1)**, seaward of P200m, bars were frequently observed in the three regions. Furthermore, the locations of the bar crests in the three regions agree very well, and so do the elevations. Shoreward of P200m, on the other hand, bars were sometimes observed only along HORS. This seems to be caused by scours around two pilings at P160m; the eroded sediment was transported seaward and formed a small bar. Nevertheless, away from HORS, the sediment was also accumulated around P180m, and the beach profiles away from HORS were similar to those along HORS. As a result, the topographies on and around the bar crests are thought to have been uniform alongshore and had little influence of the pilings of HORS.

In the troughs, on the other hand, elevations along HORS are deeper than those away from HORS as shown in **Figure 6 (2)**. This is considered to be caused by local scours, and to result in the large standard deviation along HORS from P200m to P400m shown in **Figure 4**. Even though elevations in the troughs along HORS are lower than those away from HORS, the locations of the troughs along HORS agree with those away from HORS. This means the locations of the troughs were not much influenced by scours.

Through the investigations above, the following results were found: a) the topography around HORS was generally uniform alongshore, b) on and around the bar crests, the influence of the pilings was negligible, and c) although elevations of the troughs along HORS were lower than those away from HORS, the locations of the troughs along HORS agreed well with those away from HORS. With these findings, it is concluded that the beach profile changes represented by bar movements at HORS were not much disturbed by scours of the pilings.

This conclusion is similar to that for the Field Research Facility (FRF) in the United States shown by Miller et al. (1983). The FRF is a field observation pier having a 561 m length, and is located on the Atlantic Ocean in Duck, North Carolina. Miller et al. (1983) investigated beach profile changes along and away from the FRF with the empirical eigenfunction analysis, and concluded that the beach profile change along the FRF represented by bar movement was not disturbed by the pilings. The FRF is supported by double pilings, while HORS is supported by single pilings. Hence, the conclusion that the beach profile change at HORS was not much influenced by the pilings is reasonable.

4. Results

4.1 Medium-term Bar Movement

Figure 7 shows a space-time map of the variation from the time-averaged beach profile at HORS from 1987 to 1994. Warm colors correspond to the elevations above the time-averaged profile, and cold colors to the elevations below that. The scale in the upper figure is different from that in the lower one. Although accumulations and erosions occurred alternatively with time shoreward of P150m, accumulated areas seaward of P150m repeatedly moved seaward with a period of about a year.

Then, the difference between the beach profile changes in the seaward and the shoreward regions was investigated with the power spectrum analysis applied to the elevations at P0m and P300m, which were selected as representative points in the shoreward and the seaward regions, respectively. **Figure 8** shows that the power spectrum at P0m has a broad peak over periods of about 300 to 500 days and a sharp peak at a period of 190 days, while the spectral density at P300m is concentrated at a period of a year.

Next, the bar crest migration was investigated. **Figure 9** displays that seaward of P200m, the bar crest repeatedly migrated seaward with a period of a year in particular from 1987 to 1992. That is, the bar crest generated at around P180m migrated seaward and reached the tip of HORS about a year after the beginning of the migration. Almost at the same time when the bar crest reached the tip of HORS, a new bar crest was generated at around P180m and started to migrate seaward again.

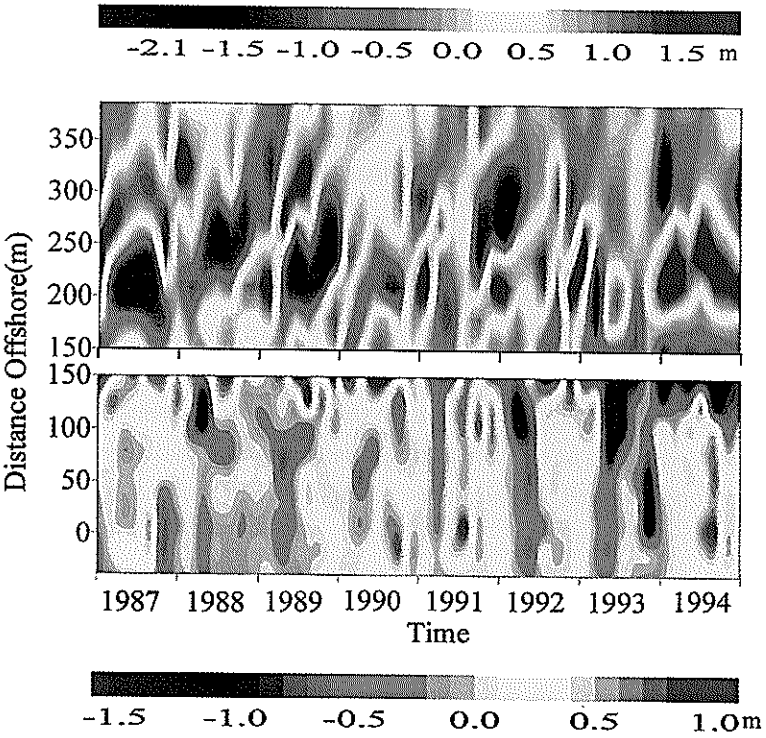

Figure 7 Variation from the mean beach profile at HORS.

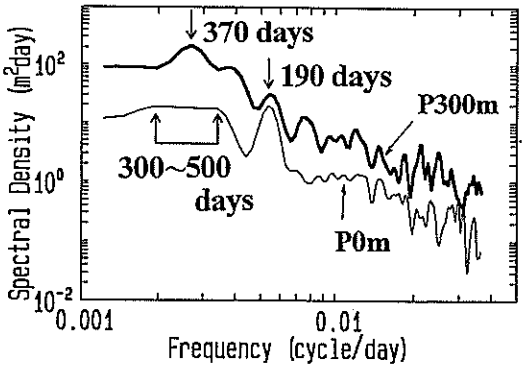

Figure 8 Power spectra of elevations at P0m and P300m.

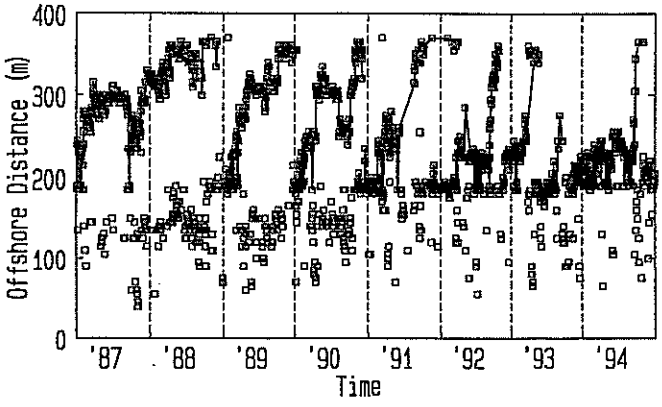

Figure 9 Bar crest migration.

Since no bars were observed seaward of P450m as shown in **Figure 6 (1)**, a bar crest is expected to migrate seaward and disappear shortly after reaching the tip of HORS. Hence, the duration time of the bar crest migration at HORS is assumed to be almost equal to the return period of the bar crest migration. According to the results of Shand and Bailey (1999), however, the duration time is longer than the return period in eight out of nine investigated coasts.

4.2 Bar Movement and Beach Profile Change in the Foreshore

The empirical eigenfunction analysis was applied to the beach profiles at HORS from which the mean beach profile had preliminarily been removed. **Figures 10 (1)** to **(3)** show the first three eigenfunctions and the temporal weightings on the eigenfunctions; the variances explained by the three eigenfunctions from the first are 42 %, 28 % and 8 %. The first two eigenfunctions are large seaward of P150m, while the third one is large even at around P0m. **Figure 11** shows the cross-shore distribution of the variance at each location explained by the first three eigenfunctions. These results indicates that the first two eigenfunctions and the third one represent beach profile changes in the nearshore and in the foreshore, respectively.

Then, the temporal weightings on the first and the third eigenfunctions were compared with parameters representing beach profile changes in the nearshore and in the foreshore, respectively. As a parameter for beach profile changes in the foreshore, the shoreline position at the high tide was chosen. The other parameter, which represents beach profile changes in the nearshore, is the difference, Δh, between the averaged water depth over the region from P270m to P380m, h_2, and that over the region from P270m to P380m, h_1; $\Delta h=h_2-h_1$. A positive value of Δh means that the sediment is accumulated seaward of P270m. **Figure 12 (1)** shows that the correlation between C_1 and Δh is very high. The correlation between C_3 and the shoreline position from the mean is also high as shown in **Figure 12 (2)**, while the correlation coefficient between C_3 and the shoreline position from the mean is lower than that between C_1 and Δh. Consequently, the first and the third eigenfunctions are confirmed to represent beach profile changes in the nearshore and in the foreshore, respectively.

The second eigenfunction, e_2, has a phase difference of $\pi/2$, one fourth of the wavelength, with the first eigenfunction, e_1, as shown in **Figures 10 (1)** and **(2)**. The temporal weighting on the second eigenfunction, C_2, also has a phase difference of $\pi/2$ with that on the first eigenfunction, C_1, as shown by the cross spectra between C_1 and C_2 in **Figure 13**. Wijnberg and Wolf (1994) showed that the superposition of two eigenfunctions with a phase difference of $\pi/2$ in their shapes and temporal weightings represents a bar crest migration, a progressive wave motion. Beach profile changes at HORS reconstructed by the first two eigenfunctions and the first eigenfunction (variances from the mean beach profile) are shown in **Figures 14 (1)** and **(2)**, respectively. The superposition of the first two eigenfunctions at HORS also represents the seaward migration of the bar crest in the nearshore (**Figure 14 (1)**), while the first eigenfunction represents a standing wave component of the beach profile change caused by the sediment movement between the region from P180m to P270m and that from P275m to P380m (**Figure 14 (2)**).

4.3 Bar Movement and Sediment Transport

To examine sediment transport rates associated with the medium-term bar crest migration, low frequency components (<0.0017 cycle/day, >60 days) of cross-shore sediment transport rates on three locations, P210m, P260m and P310m, were investigated. **Figure 15** shows the low frequency components together with the bar crest migration. The transport rates were estimated with the beach profiles reconstructed by the first two eigenfunctions on the basis of two assumptions. One is that the beach profile change was not influenced by the longshore sediment transport. The other is that the cross-shore sediment transport rate was zero at P-115m, the shoreward limit of the survey area and located at the foot of a dune. The porosity was assumed to be 0.4, and the shoreward sediment transport was defined to be positive.

Although the bar crest migrates in one direction, seaward, the cross-shore sediment transport rates fluctuate shoreward and seaward. Furthermore, there are phase differences among the transport rates; the fluctuation at P210m

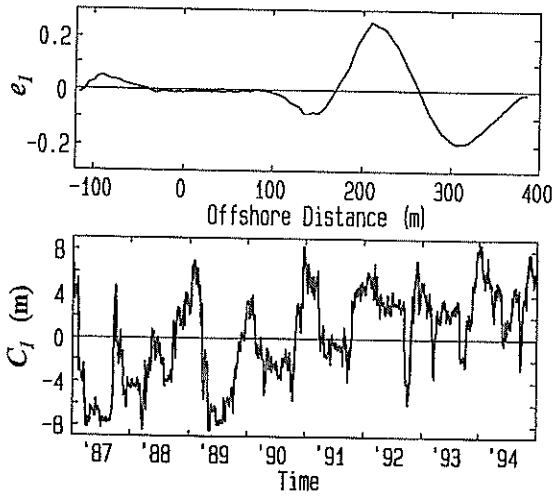

Figure 10 (1) The first eigenfunction, e_1 and its temporal weighting, C_1.

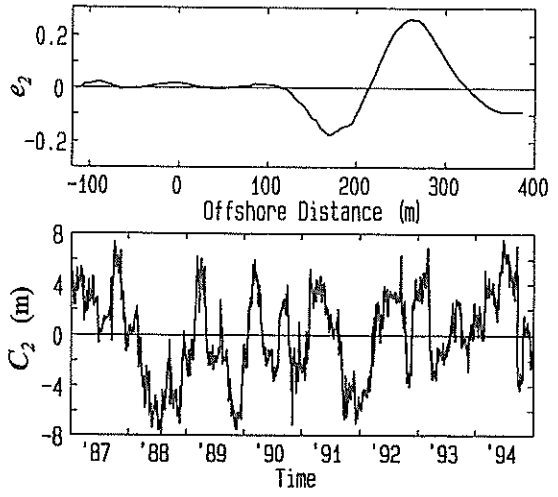

Figure 10 (2) The second eigenfunction, e_2 and its temporal weighting, C_2.

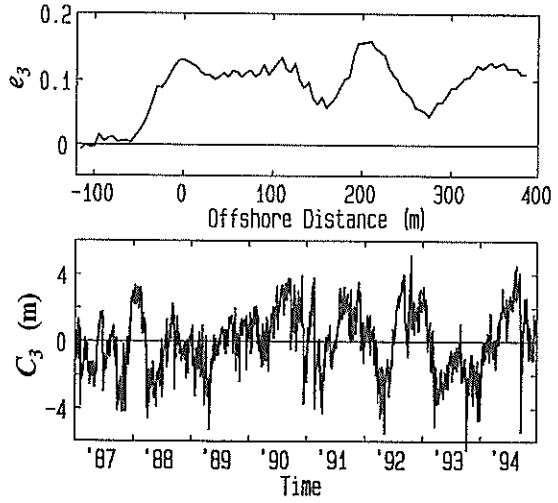

Figure 10 (3) The third eigenfunction, e_3 and its temporal weighting, C_3.

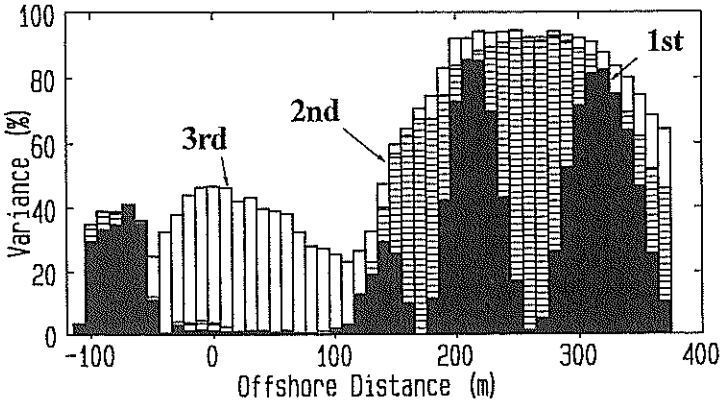

Figure 11 Variance at each location explained by the first three eigenfunctions

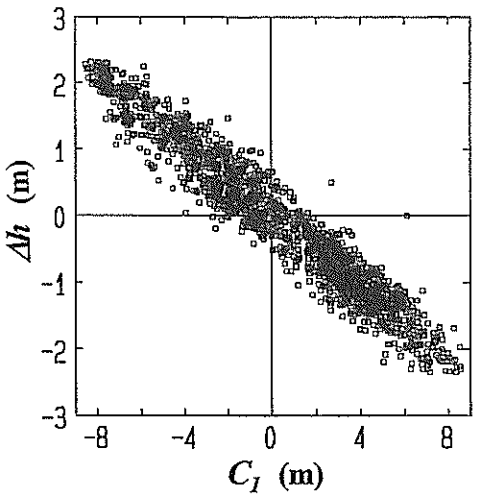

Figure 12 (1) Relationship between C_1 and Δh.

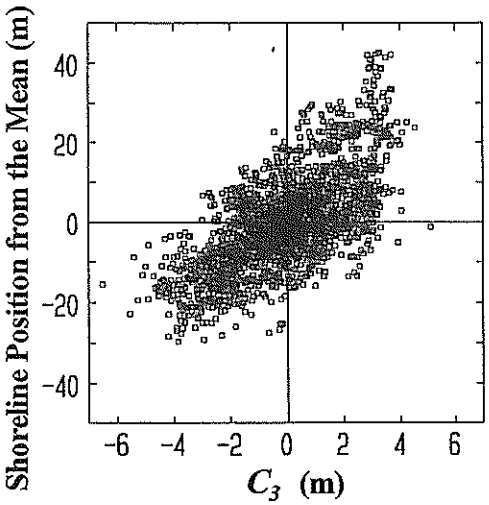

Figure 12 (2) Relationship between C_3 and the shoreline position from the mean.

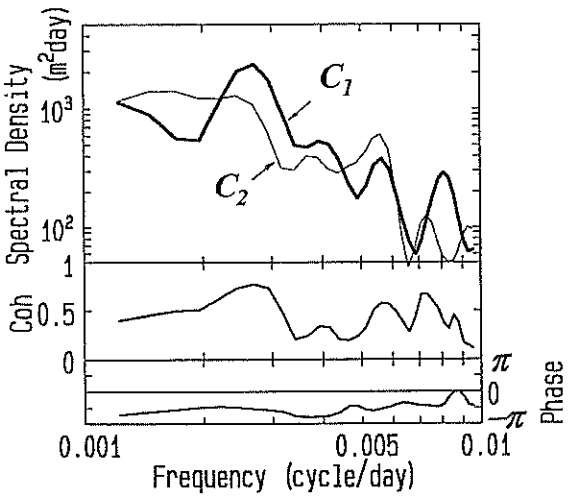

Figure 13 Cross spectra between C_1 and C_2.

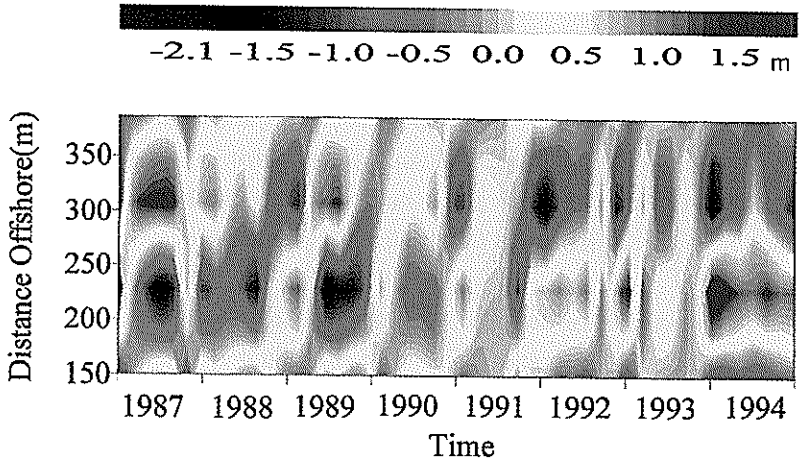

Figure 14 (1) Beach profile change at HORS reconstructed by the first two eigenfunctions.

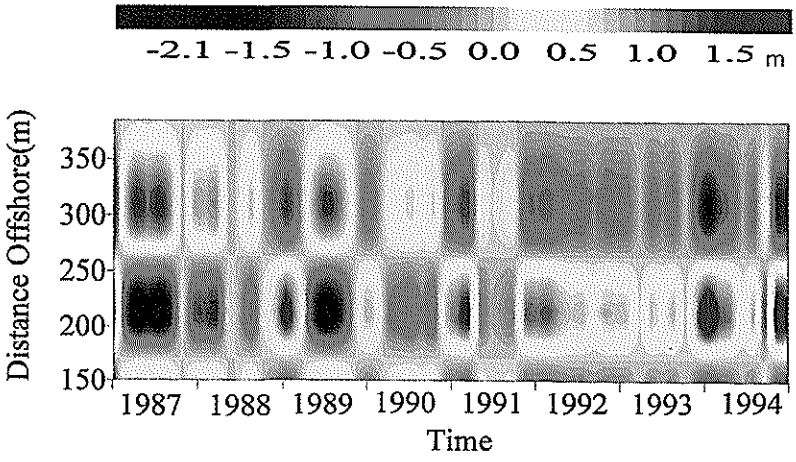

Figure 14 (2) Beach profile change at HORS reconstructed by the first eigenfunction.

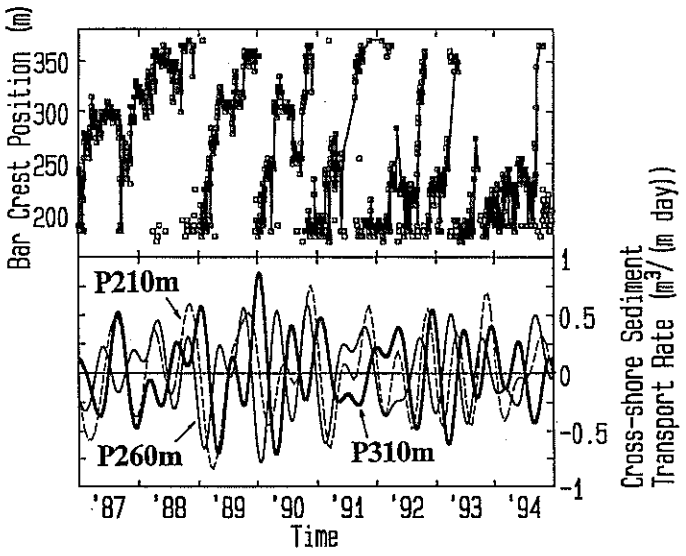

Figure 15 Low frequency components of cross-shore sediment transport rates and bar crest migration.

is earlier than that at P260m by $\pi/4$, while that at P310m is later than that at P260m by $\pi/4$.

Then, cross-shore distributions of the low frequency component of the cross-shore sediment transport rate were examined. **Figure 16** shows that seaward sediment movement occurred on and around the bar crests, even though shoreward sediment movement temporally occurred there in August as shown in (b). In the trough regions, on the contrary, shoreward sediment movement occurred. The phase differences among the cross-shore sediment transport rates shown in **Figure 15** is thought to be attributed to the differences of the times when the bar crests reached the locations.

Figure 16 also shows the development and the decay of a bar during the seaward bar crest migration; the bar was developed in the first half of the bar crest migration, and was attenuated in the second half. The cross-shore distribution of the bar height averaged over the eight years is shown in **Figure 17**; the offshore distance of a bar was defined to be the mean value of the distances at the bar crest and at the trough. The bar height gets larger from P200m to P250m, has a peak at around P250m, and then gets smaller to P380m like the bar shown in **Figure 16**. This distribution is likely caused by the cross-shore distribution of the cross-shore sediment transport rate. Hence, the root-mean-square value of the cross-shore sediment transport rate at each survey point was calculated with the time-series of the transport rate; the transport rate was estimated on the basis of the beach profiles reconstructed by the first two eigenfunctions. **Figure 18** shows that the root-mean-square value of the cross-shore sediment transport rate rapidly increases from P150m to P250m, and then gradually decreases. This distribution is similar to that of the bar height. This means that the bar was developed to P250m because the magnitude of the cross-shore sediment transport rate increased, while the bar was attenuated because the magnitude decreased.

4.4 Sediment Transport and Wave Energy

As a parameter representing the overall sediment transport seaward of P150m, the moving velocity of the cross-shore location of a mass center from P150m to P380m, V_c, was taken. The mass center was estimated on the basis of the variations from the mean beach profile; the variations were reconstructed by the first two eigenfunctions. Since the cross-shore sediment transport rate was small at P150m (**Figure 18**), a positive value of V_c means that sediment seaward of P150m was generally transported seaward.

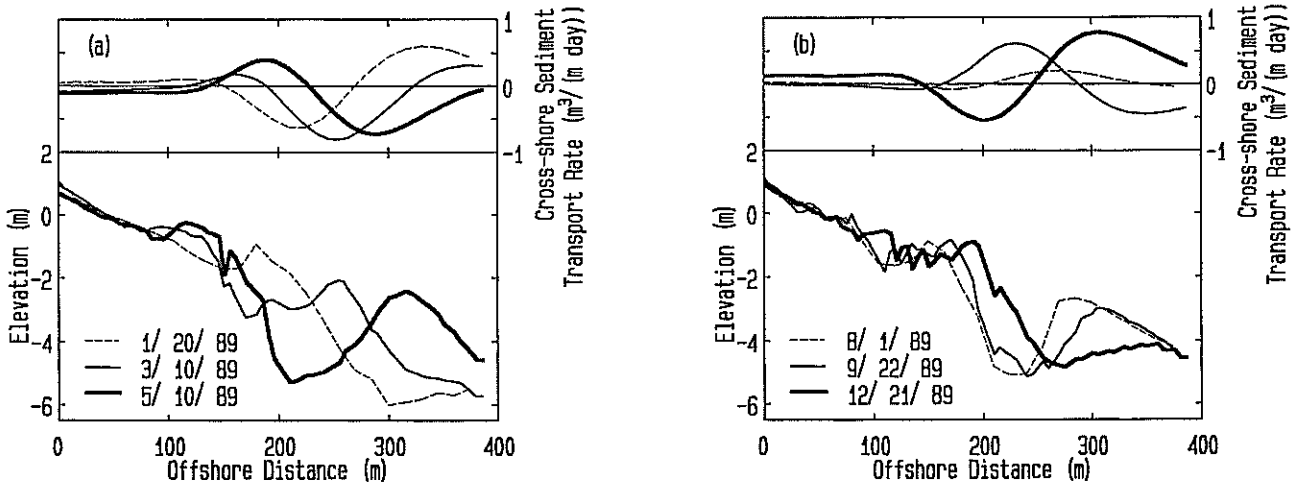

Figure 16 Cross-shore distributions of low frequency component of cross-shore sediment transport rate (upper parts) and beach profiles (lower parts) during (a) the first half of the seaward bar crest migration and (b) the second half.

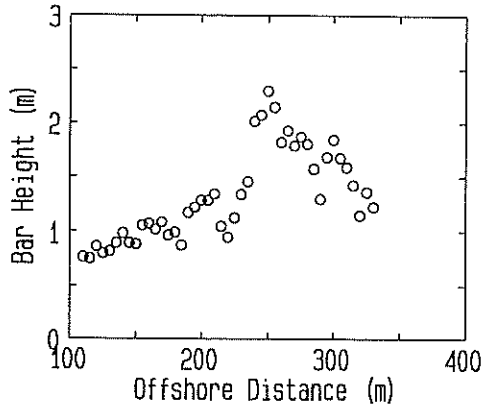

Figure 17 Cross-shore distribution of bar height.

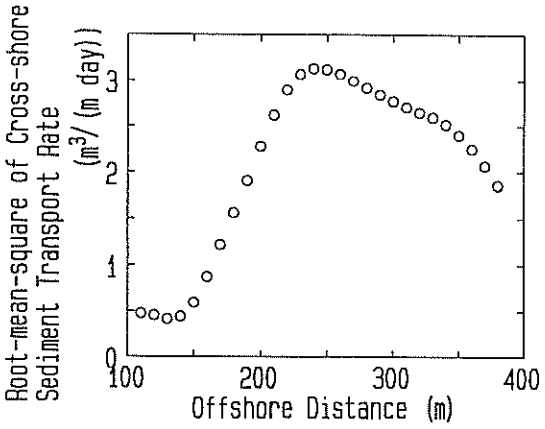

Figure 18 Cross-shore distribution of root-mean-square value of cross-shore sediment transport rate.

Before the investigation on the relationship between V_c and wave energy, the characteristics of V_c was examined. **Figure 19 (1)** shows the correlation between V_c and the cross-shore sediment transport rate at P260m, Q_{260}, and **Figure 19 (2)** shows the correlation between V_c and dC_1/dt, which represents morphological change in the nearshore.

The correlation between V_c and Q_{260} was expected to be low because in contrast with Q_{260}, which represents the sediment transport rate just at one location, V_c was estimated with the consideration of all sediment movements seaward of P150 and thus reflects phase differences among the transport rates as shown in **Figure 15**. **Figure 19 (1)**, however, shows that V_c and Q_{260} has a strong correlation. The reason is that the sediment transport at P260m was predominant seaward of P150m as shown in **Figure 18**.

The correlation between V_c and dC_1/dt is also high (**Figure 19 (2)**). This means that while the first eigenfunction cannot represent the seaward bar crest migrations well because an eigenfunction represents only a standing wave motion, it can represent the sediment movements associated with the bar crest migrations.

Then, the parameter V_c was investigated with the wave energy flux in deep water, E_f, which was estimated with Eq. (1) on the basis of wave data obtained offshore of Kashima Port; the location of the wave gage is shown in Figure 1, and the water surface elevations were measured for twenty minutes every two hours.

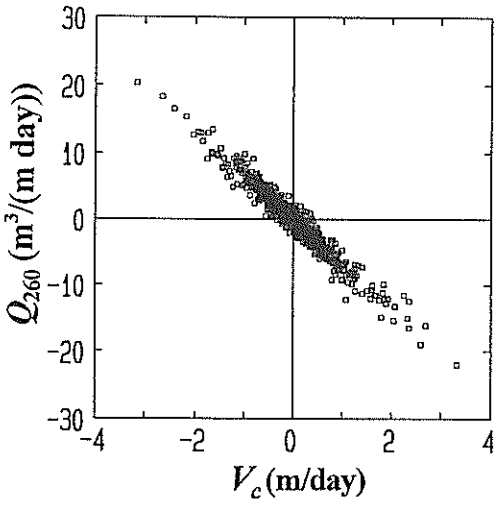

Figure 19 (1) Relationship between V_c and Q_{260}.

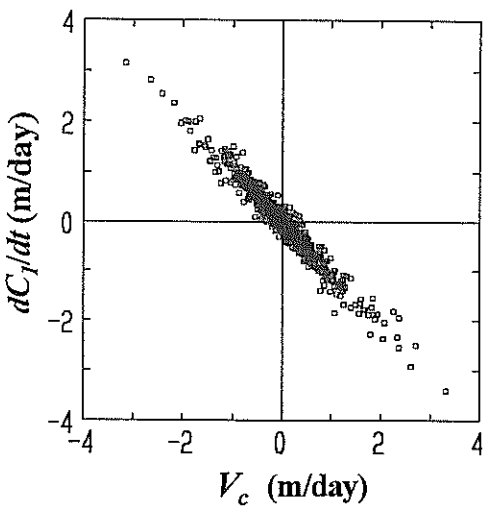

Figure 19 (2) Relationship between V_c and dC_1/dt.

$$E_f = \frac{1}{8}\rho g H_{0,1/3}^{\ 2} C_g \ , \tag{1}$$

where ρ is the density of sea water, g is the gravity acceleration, $H_{0,1/3}$ is the offshore significant wave height, and C_g is the group velocity.

Figure 20 (1) shows the cross spectra between the absolute value of V_c and E_f. The coherence is high, and the phase difference is almost 0. This means that the overall sediment movement was active when the offshore wave energy flux was large.

The cross spectra between V_c and E_f are shown in **Figure 20 (2)**. The coherence is high at periods of a year and six months, and the phase difference is $\pi/2$ at a period of a year and $-\pi/2$ at a period of about six months. **Figure 21 (1)** compares the time-series of the low frequency components (<0.006 cycle/day, >160 days) of V_c and E_f, and **Figure 21 (2)** shows the mean seasonal changes of V_c and E_f obtained with the low frequency components. In V_c, the spectral density at a period of a year is larger than that at a period of six months (**Figure 20 (2)**), and hence the variation with a period of a year is predominant (**Figure 21 (1)**), while the amplitude of the variation with a period of six months increases from 1992. In E_f, on the other hand, since the density at a period of a year is almost equal to that at a period of six months (**Figure 20 (2)**), the variation of E_f has two peaks in a year (**Figure 21 (1)**). Because a positive V_c means that the sediment is generally transported seaward, the variations of V_c and E_f shown in **Figure 21 (2)** indicates that in

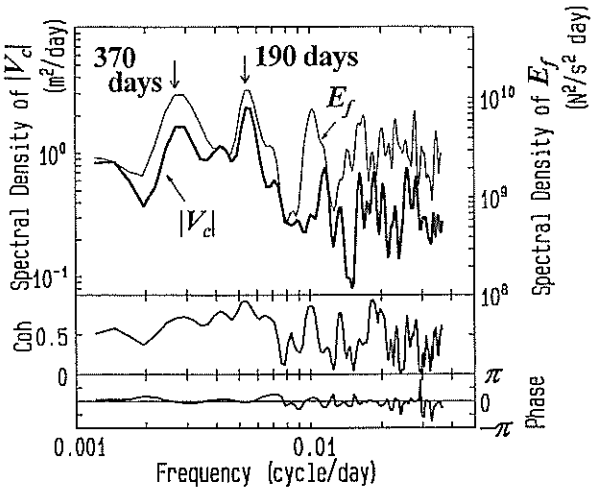

Figure 20 (1) Cross spectra between $|V_c|$ and E_f.

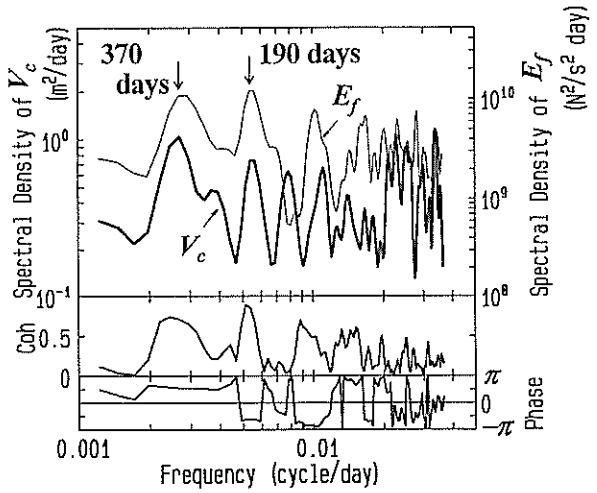

Figure 20 (2) Cross spectra between V_c and E_f.

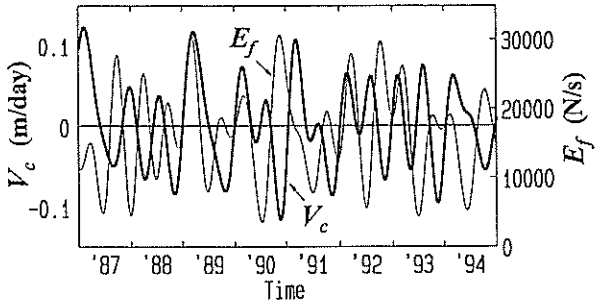

Figure 21 (1) Low frequency components of V_c and E_f.

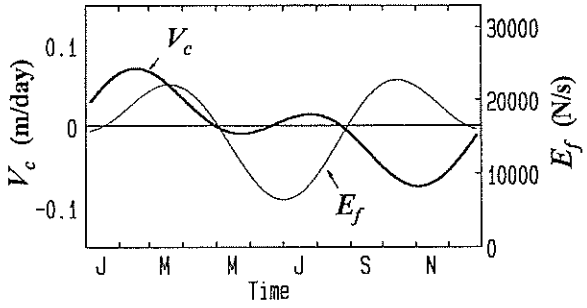

Figure 21 (2) Seasonal change of V_c and E_f.

the region from P150m to P380m, the sediment accumulated at around P180m was transported seaward from winter to spring, when developed depressions induced high waves, and was accumulated offshore. Then, the sediment moved shoreward in autumn, when typhoons stroke Japan and caused high waves, and was accumulated at around P180m.

5. Discussion

The seaward migration of the bar crest at HORS shown in **Figure 9** is similar to those on several coasts in the United States, the Netherlands and New Zealand (Birkemeier, 1984; Lippmann et al., 1993; Ruessink and Kroon, 1994; Wijnberg and Terwindt, 1995; Shand and Bailey, 1999), while the Hasaki Coast, where HORS is located, basically has a single bar in contrast with the other coasts having multi bars. The seaward bar crest migration at HORS is also explained like the others by the conceptual model of Ruessink and Kroon (1994), which consists of generation, seaward migration and degeneration of a bar.

Table 1 lists the duration time of the seaward bar migration, the nearshore and the foreshore slopes, the mean wave height and period, and the wave height in storm at Hasaki and three other coasts on the basis of Shand and Bailey (1999) and Shand et al. (1999). The wave height in storm was defined to be the height of which the nonexceedance probability is 0.99. The statistical values of wave climate were estimated on the basis of the daily-averaged significant wave height.

The duration time at Hasaki is shorter than that in the Netherlands, and this difference is similar to the results of Shand et al. (1999). Shand et al. (1999) investigated the relationships between the duration time of the seaward bar crest migration and hydrodynamic and morphological properties, and showed that the long duration time corresponds to the mild nearshore slope. They assumed that a beach with the mild slope tends to be exposed to high waves, which generate a large bar requiring long time for the seaward migration. Other than this assumption, there is another explanation that when the water depth of the bar disappearance is assumed to be fixed, on a beach with the mild slope, the distance along which a bar crest migrates gets long; the long distance results in the long duration time. Furthermore, in the Netherlands, where multiple bars exist, low waves generated by the energy dissipation on an offshore bar may drop the speed of the shoreward bar migration as suggested by Ruessink and Terwindt (2000).

Although the difference between the duration time of the bar crest migration at Hasaki and that in the Netherlands can be explained by the difference in the nearshore slope, the difference between the duration time at Hasaki and those at Duck and Wanganui cannot be explained by the nearshore slope. According to the nearshore slope, the time at Hasaki would be longer than those at Duck and Wanganui. Other factors such as longshore current affect the duration time (Shand et al., 1999).

Table 1 Duration time of bar crest migration, and morphological and wave characteristics

Location	Duration Time (year)	Nearshore Slope	Foreshore Slope	Mean Wave Height (m)	Mean Wave Period (s)	Wave Height in Storm (m)
The Netherlands	6～20	0.004～0.008	0.015～0.02	1.35	6.0	4.1～4.3
Duck, USA	4	0.0097	0.052～0.060	1.10	6.4	3.05
Wanganui, New Zealand	2～5	0.0083～0.0092	0.029～0.031	1.20	7.8	3.20
Hasaki, Japan	1	0.008	0.02	1.37	8.0	4.36

The empirical eigenfunction analysis applied to the beach profiles at HORS separated the topography change in the nearshore from that in the foreshore as shown in **Figures 10 (1)** to **(3)**, while these were rarely separated in previous studies (*e.g.* Winant et al., 1975; Aubrey, 1979; Birkemeier, 1984; Wijnberg and Terwindt, 1995). This separation means that the beach profile change in the foreshore at HORS was almost independent of the bar movement. Takeda and Sunamura (1992), however, showed that the shoreline with a bar close to it is less retreated than that with a bar away from it. Hence, the influence of the bar on the shoreline movement at HORS was examined with the same method as Takeda and Sunamura (1992) taken. Using a parameter C_s defined by the following equation, they investigated the critical condition to distinguish shoreline advance and retreat on the basis of field data with bars at various locations.

$$C_S = \frac{H_0}{L_0^{0.33}} (\tan\beta)^{-0.27} d^{-0.67}, \tag{2}$$

where H_o is the offshore wave height, L_0 is the offshore wavelength corresponding to the offshore wave period, $\tan\beta$ is the beach slope from the shoreline to a water depth of 20 m, and d is the sediment diameter.

The shoreline movements at HORS in which the retreat speed of the shoreline was larger than 2 m/day or shoreline advance continued more than three days were picked up, and the values of C_s in the shoreline movements were examined with the initial shoreline positions. **Figures 22** shows the results in (a) C_f>3 and in (b) C_f<-3; a positive C_f means that a bar is located shoreward. Takeda and Sunamura (1992) adopted the maximum value of the daily averaged significant wave height as H_0 because they thought that the topography change is sensitive to the maximum value during the change. However, the accuracy of the distinction between the shoreline advance and retreat with the mean significant wave height is better than that with the maximum value. Thus, as H_0, this study employed the mean significant wave height. The value of $\tan\beta$ is set to be 1/120, and d is 0.2mm.

The solid lines in the figures, obtained with discriminant analysis, show the conditions distinguishing shoreline advance and retreat. The shoreline with shoreward initial position is less retreated than that with seaward initial position. This tendency is observed both in C_f>3 and C_f<-3, and is consistent with the results of Katoh and Yanagishima (1988) and Takeda and Sunamura (1992).

The locations of the lines are similar in C_f>3 and C_f<-3. This means that the bar at HORS had little influence on the shoreline movement. The difference between the results of this study and of Takeda and Sunamura (1992) is due to the

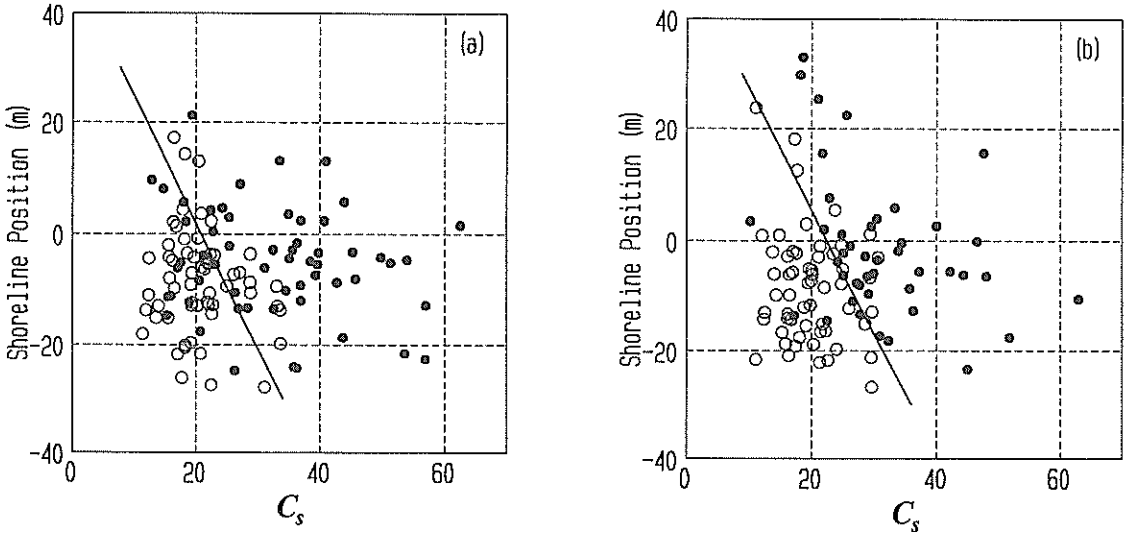

Figure 22 Initial shoreline position and C_s in shoreline advance and retreat in (a) C_f>3 and (b) C_f<-3. (Open circles show the values in shoreline advance, and solid circles show those in shoreline retreat.)

difference of the locations of the bars. They obtained the field data on the Naka Coast about 60 km north of the Hasaki Coast; the wave characteristics and the beach profiles on the two coasts are similar. They dealt with bars developed about 75 m to 200 m seaward of the shoreline although this study discussed bars more than 200 m away from the shoreline. The influence of bars near the shoreline on the topography change in the foreshore is considered to be larger than that of bars away from the shore (Takeda and Sunamura, 1992). As a result, the influence of the bar on the topography change was observed in Takeda and Sunamura (1992), and not in this study.

As described above, the bar crest migration at HORS was found to have little influence on the topography change in the foreshore. The result, however, is interpreted to be for an outer bar moving within a range where the seaward bar crest migration is repeated, in other words, "dynamic equilibrium" range. If the bar moves out of the range, the foreshore topography change corresponding to the unusual bar movement may occur. Furthermore, Stive et al. (1996) suggest a strong correlation between bar movement and the foreshore topography change. Further investigations on the relationship between bar movement and the topography change in the foreshore are required with field data obtained at various sites.

Compared with long-term and medium-term bar crest migrations, the sediment movements associated with the bar crest migrations were rarely investigated. Ruessink and Terwindt (2000) proposed a model in which knowledge on sediment movement in short-term process is expanded for the explanation of the medium-term bar movement. The model partially succeeded to reproduce the bar movement, but could not explain a bar generation process; the sediment movement in bar generation was still unknown. **Figure 23** is a schematic diagram showing the bar crest migration and the sediment movement at HORS; the sediment movements in the figure correspond to the beach profiles shown by the thick solid lines. The cross-shore distribution of the cross-shore sediment transport rate consisted of seaward sediment movement on and around a bar crest and shoreward sediment movement in a trough region. The seaward sediment movement induced the seaward bar crest migration, and the shoreward sediment movement contributed to the next bar generation.

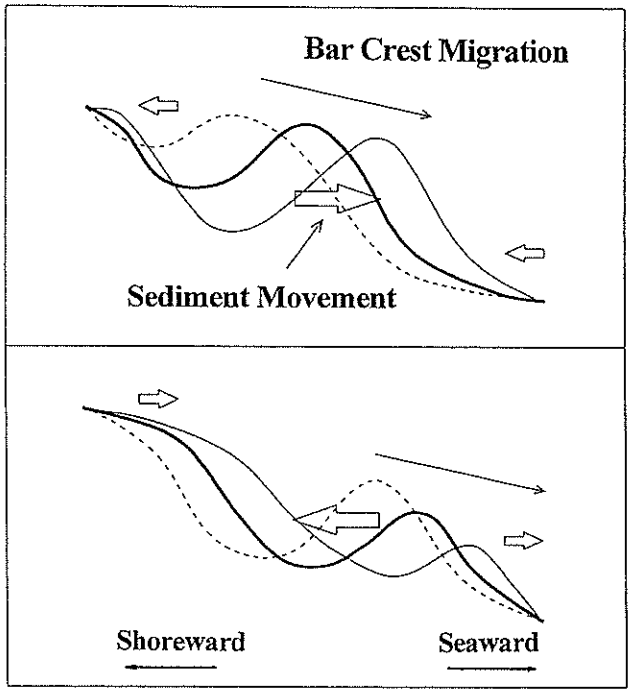

Figure 23 Schematic diagram showing the bar crest migration and the sediment movement.

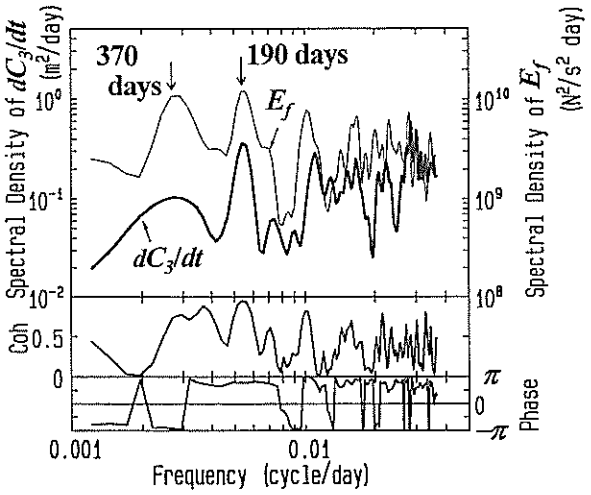

Figure 24 Cross spectra between dC_3/dt and E_f.

To examine the difference between the morphological response to the waves in the nearshore shown in **4.4** and that in the foreshore, the cross spectra between E_f and dC_3/dt, which represents morphological change in the foreshore, were calculated. **Figure 24** shows that the coherence is high at periods of a year and six months, and that the phase difference at the periods is π. This phase difference means that the foreshore was eroded when the wave height was large, while the foreshore was accumulated when the wave height was small. This morphological response is consistent with other observations (*e.g.* Katoh and Yanagishima, 1988).

In contrast with the morphological changes in the foreshore corresponding to the offshore wave heights, those in the nearshore differed even with similar offshore wave heights as shown in **Figure 21 (2)**; the sediment in the nearshore moved seaward under severe wave conditions from winter to spring, did not move under mild wave conditions in summer, and returned shoreward under severe wave conditions in autumn. Although the wave conditions from winter to spring and in autumn were similar, the locations of the bars were different; the bars in autumn were located seaward than those from winter to spring. As a result, the area around P260m, at which the sediment movement was predominant (**Figure 18**) and controlled the overall sediment transport seaward of P150m (**Figure 19 (1)**), was located around the bar crests from winter to spring and in the trough regions in autumn. The wave energy around P260m in autumn was smaller than that from winter to spring owing to the wave energy dissipation on the seaward bars, and hence induced the shoreward sediment movement.

6. Conclusions

The beach profile data obtained from the foot of a dune to a water depth of about 5 m at HORS showed that a bar crest repeatedly migrated seaward from around P180m with a period of a year. The duration time, which is almost equal to the return period, is shorter than those on coasts in the United States, the Netherlands, and New Zealand. The difference between the duration time at HORS and that in the Netherlands was explained by the difference in the nearshore slope as shown by Shand et al. (1999), though the difference between the duration time at HORS and those in the United States and New Zealand was not explained by the difference in the slope.

The empirical eigenfunction analysis and the investigation on the shoreline movement revealed that the bar movement at HORS had little influence on the topography change in the foreshore. This may be because the bar movement at HORS was within a range where the seaward bar movement was repeated.

Although the bar crest migrated almost in one direction, seaward, the cross-shore sediment transport associated with the bar crest migration fluctuated seaward and shoreward. Seaward sediment transport occurred on and around a bar

crest and induced the seaward migration of the bar crest, while shoreward sediment transport occurred in a trough region and contributed to the next bar generation.

The overall sediment movement seaward of P150m, mainly controlled by the sediment movement at P260, is that the sediment was transported seaward by high offshore waves from winter to spring, and returned shoreward by those in autumn. This result indicates that in contrast with the sediment movement in the foreshore corresponding to the offshore wave height, the sediment in the nearshore was transported not only seaward and but also shoreward under similar severe wave conditions offshore. This is probably because the locations of the bars were different. The bars in autumn located seaward than those from winter to spring reduced the wave energy around P260m, located in the trough regions in autumn. The reduced wave energy resulted in the shoreward sediment movement.

(Received on August 31, 2000)

Acknowledgements

The author appreciates critical reviews by Dr. Y. Hosokawa and Ms. A. Veltcheva, and comments of Drs. K. Katoh, S. Takahashi and N. Hashimoto, and Prof. K. Nadaoka. The offshore data were provided by Kashima Port Construction Office of the Second District Port Construction Bureau, Ministry of Transport, and Marine Observation Laboratory of Port and Harbour Research Institute. Special thanks are extended to all the staff members at HORS, who have been conducting field surveys even in storms.

References

Aagaard, T. and Greenwood, B. (1999): Directionality cross-shore sediment transport in the surf zone under high-energy conditions, *Coastal Sediments '99*, ASCE, pp.1003-1018.

Aubrey, D.G. (1979): Seasonal patterns of onshore/offshore sediment movement, *J. Geophys. Res.*, Vol.84, No.C10, pp.6347-6354.

Birkemeier, W.A. (1984): Time scales of nearshore profile changes, *Proc. 19th Coastal Eng. Conf.*, ASCE, pp.1507-1521.

Gallagher, E.l., Elgar, S. and Guza, R.T. (1998): Observations of sand bar evolution on a natural beach, *J. Geophys. Res.*, Vol.104, No.C7, pp.3203-3215.

Greenwood, B. and Osborne, P.D. (1991): Equilibrium slopes and cross-shore velocity asymmetries in a storm-dominated, barred nearshore system, *Marine Geology*, 96, pp.211-235.

Komar, P. A. (1998): Beach Processes and Sedimentation, Second Edition, Prentice-Hall Inc., 544p.

Katoh, K. and Yanagishima, S. (1988): Predictive model for daily changes of shoreline, *Proc. 21st Coastal Eng. Conf.*, ASCE, pp.1253-1264.

Kuriyama, Y. (1996): Cross-shore movements of longshore bars, *Proc. Coastal Engineering*, JSCE, Vol.43, pp.576-580. *(in Japanese)*

Larson, M. and Kraus, N.C. (1992): Dynamics of longshore bars, *Proc. 23rd Coastal Eng. Conf.*, ASCE, pp.2219-2232.

Larson, M. and Kraus, N.C. (1994): Temporal and spatial scales of beach profile change, Duck, North Carolina, *Marine Geology*, 117, pp.75-94.

Larson, M., Capobianco, M., and Hanson, H. (2000): Relation-ship between beach profiles and waves at Duck, North Carolina, determined by canonical correlation analysis, *Marine Geology*, 163, pp.275-288.

Lippmann, T.C. and Holman, R.A. (1990): The spatial and temporal variability of sand bar morphology, *J. Geophys. Res.*, Vol.95, No.C7, pp.11575-11590.

Lippmann, T.C., Holman, R.A. and Hathaway, K.K. (1993): Episodic, nonstationary behavior of a double bar system at Duck, North Carolina, U.S.A., 1986-1991, *J. Coastal Res.*, Special Issue 15, pp.49-75.

Miller, H.C., Birkemeier, W.A. and DeWall, A.E. (1983): Effects of CERC research pier on nearshore processes,

Coastal Structure '93, pp.769-784.

Miller, H.M., Smith, S.J., Hamilton, D.G. and Resio, D.T. (1999): Cross-shore transport processes during onshore bar migration, *Coastal Sediments '99*, ASCE, pp.1065-1080.

Plant, N.G. and Holman, R. (1997): Strange kinematics of sand-bars, *Coastal Dynamics '97*, ASCE, pp.355-364.

Plant, N.G., Holman, R.A. and Freilich, M.H. (1999): A simple model for interannual sandbar behavior, *J. Geophys. Res.*, Vol.104, No.C7, pp.15755-15776.

Ruessink, B.G. and Kroon, A. (1994): The behaviour of a multiple bar system in the nearshore zone of Terschelling, the Netherlands: 1965-1993, *Marine Geology*, 121, pp.187-197.

Ruessink, B.G. and Terwindt, J.H.J. (2000): The behaviour of nearshore bars on the time scale of years: a conceptual model, *Marine Geology*, 163, pp.289-302.

Sallenger, Jr., A.H., Holman, R.A. and Birkemeier, W.A. (1985): Storm-induced response of a nearshore-bar system, *Marine Geology*, 64, pp.237-257.

Sallenger, Jr., A.H. and Howd, P.A. (1989): Nearshore bars and the break-point hypothesis, *Coastal Eng.*, 12, pp.301-313.

Shand, R.D. and Bailey, D.G. (1999): A review of net offshore bar migration with photographic illustrations from Wanganui, New Zealand, *J. Coastal Res.*, Vol.15, No.2, pp.365-378.

Shand, R.D., Bailey, D.G. and Shepherd, M.J. (1999): An inter-site comparison of net offshore bar migration characteristics and environmental conditions, *J. Coastal Res.*, Vol.15, No.3, pp.750-765.

Stive, M.J.F., Guillen, J. and Capobianco, M. (1996): Bar migration and duneface oscillation on decadal scales, *Proc. 25th Coastal Eng. Conf.*, ASCE, pp.2884-2896.

Sunamura, T. and Takeda, I. (1993): Bar movement and shoreline change: Predictive relations, *J. Coastal Res.*, Special Issue 15, pp.125-140.

Takeda, I. and Sunamura, T. (1992): Conditions for beach erosion on a barred beach, *Zeit. Geomorph. N.F.*, 36, 4, pp.453-464.

Thornton, E.B., Humiston, R.T. and Birkemeier, W. (1996): Bar/trough generation on a natural beach, *J. Geophys. Res.*, Vol.101, No.C5, pp.12097-12110.

Wijnberg, K.M. and Wolf, F.C.J. (1994): Three-dimensional behaviour of a multiple bar system, *Coastal Dynamics '94*, pp.59-73.

Wijnberg, K.M. and Terwindt, J.H.J. (1995): Extracting decadal morphological behaviour from high-resolution, long-term bathymetric surveys along the Holland coast using eigenfunction analysis, *Marine Geology*, 126, pp.301-330.

Winant, D.C., Inman, D.L. and Nordstrom, C.E. (1975): Description of seasonal beach changes using empirical eigenfunction, *J. Geophys. Res.*, Vol.80, No.15, pp.1979-1986.

Yamamoto, K. and Sato, S. (1998): Large wave tank experiments on bar and berm formation due to irregular waves, *Proc. Coastal Engineering*, JSCE, Vol.45, pp.526-530. *(in Japanese)*